PAPER

Spin waves in quantum gases—the quality factor of the identical spin rotation effect

IOP Publishing Physica Scripta
Phys. Scr. 93 (2018) 094002 (8pp) https://doi.org/10.1088/1402-4896/aad4d6

Spin waves in quantum gases—the quality factor of the identical spin rotation effect

L Lehtonen[1], O Vainio[1], J Ahokas[1], J Järvinen[1], S Sheludyakov[1,3], K-A Suominen[1], S Vasiliev[1], V Khmelenko[2] and D M Lee[2]

[1] Department of Physics and Astronomy, University of Turku, FI-20014 Turku, Finland
[2] Institute for Quantum Science and Engineering, Department of Physics and Astronomy, Texas A&M University, College Station, TX, 77843, United States of America

E-mail: laanle@utu.fi

Received 11 May 2018, revised 11 July 2018
Accepted for publication 20 July 2018
Published 8 August 2018

Abstract

Our recent experimental work on electron spin waves in atomic hydrogen gas has prompted a revisit of the theory of the identical spin rotation effect (ISRE). A key characteristic determining the properties of the spin waves is the quality factor of ISRE. Unfortunately, calculating this quality factor takes some toil. In this paper we summarize some results of the ISRE theory in dilute gases. We also derive asymptotic formulae for the quality factor and examine their accuracy for hydrogen and ^{3}He.

Supplementary material for this article is available online

Keywords: spin waves, identical spin rotation, atomic hydrogen

(Some figures may appear in colour only in the online journal)

1. Introduction

Studies of quantum gases have been an integral part of quantum optics for several decades. The ground state of spin-polarized atomic hydrogen forms an interesting four-level system that can be controlled by NMR (nuclear spin) and ESR (electron spin) methods. The role of atomic collisions, however, can be very different in this system compared to laser spectroscopy or cooling of atoms. The key point is that atomic collisions can lead to other collective spin phenomena such as spin waves and their description with quasiparticles, the magnons. Thus it is both interesting and crucial to understand collisions in spin-polarized low-temperature hydrogen atoms. By making this study we wish to honor Professor Dr Wolfgang Schleich and his many significant contributions to quantum optics and beyond.

In the scattering of atoms, indistinguishablity and identicalness play a central role. Crucially, identical atoms in the same spin state experience interference effects, but identical atoms in orthogonal spin states behave as distinguishable atoms. The difference is particularly stark for fermions, where the difference between parallel and orthogonal spin states determines whether the lowest-order interaction is the partial p-wave or s-wave, respectively.

The result is an effective spin-dependent interaction between the atoms, known as the identical spin rotation effect (ISRE) [1]. ISRE acts between identical atoms in neither parallel nor orthogonal spin states. Its effect is a rotation of the interacting spins around their sum, an inevitable consequence of the different phase shifts that the different spin components of a superposition state experience. As an exchange effect, ISRE becomes more pronounced as the wave function overlap $\Lambda_{\rm th}$ becomes larger than the typical interaction range a_s, being significant already in the quantum gas regime ($\Lambda_{\rm th} > a_s$).

ISRE is intimately connected to transport phenomena such as heat conduction and spin diffusion. In particular, helical spin currents or spin waves have been predicted [2, 3] and observed for example in nuclear spins [4, 5] and in electron spins of atomic hydrogen [6, 7]. In electron spin spectra these spin waves modify the shape of the main absorption peak and create side peaks related to certain wave numbers. The temperature and density behavior of one of the peaks has also suggested that one may treat these spin waves

[3] Current affiliation: Institute for Quantum Science and Engineering.

as quasiparticles (magnons) which undergo Bose–Einstein Condensation [6]. Spin transport effects related with ISRE have also been observed in liquid ^{3}He [8], ^{3}He gas [9, 10], liquid ^{3}He–^{4}He mixtures [11], and in the cold gas of ^{87}Rb [12–14].

The main equations describing spin transport in quantum gases turned out to be identical with those for the degenerate Fermi liquids, e.g. in liquid ^{3}He and mixtures of ^{3}He in ^{4}He, where the spin precession occurs due to an effective molecular field [15, 16]. In fact, the theory of degenerate Fermi liquids was first used to predict and characterize spin waves in quantum gases [17]. It was later shown [18] that this similarity of the ISRE theory and the Leggett–Rice theory in Fermi liquids is not a coincidence, but a consequence of the same physical origin of spin transport phenomena in these systems.

The quality factor of the spin waves is central to characterizing the region where spin waves persist. It is a measure of the persistence of the spin waves against homogenizing diffusion, and can be given as a ratio of the spin-wave frequency to their time decay constant. Generally it is related to the spin-wave quality factor μ, a ratio measuring the effect of ISRE to classical diffusion. In the case of the spin-$1/2$ gas the quality factor of spin waves is given by $|\mu S|$, where S stands for the spin polarization density of the unperturbed spin gas. For higher spins one may have different results [19]. Couplings to other degrees of freedom may also significantly reduce the actual quality factor [3]. These issues are elaborated on in section 2.

The calculation of the spin-wave quality factor μ is quite complicated [20], generally involving various scattering quantities at different momenta and their averages. However at low temperatures only the s-wave scattering contributes significantly to the interactions (for both bosons and fermions, as ISRE ultimately occurs between non-parallel states). From heuristic arguments it has been known that $\mu \sim \frac{\Lambda_{\rm th}}{a_s}$ as $T \to 0$, where the right-hand side is simply proportional to the 'quantumness' of the gas. The asymptotic limit of μ was first derived in [18]; in section 3, we repeat this derivation with more detail. For comparison, an expression with higher-order terms is also derived. With this as a basis, we derive the asymptotic limit for μ of electron spin waves based on the approach of Bouchaud and Lhuillier [3], who considered specifically the case of b–c-coherence in atomic hydrogen and treated hydrogen explicitly as composed of a nucleus and an electron. Finally, in section 4 the accuracy of these expressions as compared against a numerical calculation of μ for hydrogen and ^{3}He is provided.

2. Types of ISR equations

The ISR equation is a spin diffusion equation which accounts for spin currents arising from symmetrization of wave functions. The first step in its derivation is to derive the relevant scattering cross section(s), first done by Pinard and Laloë [21] and later repeated in [1, 22]. In the second step, the cross section is used in a Boltzmann equation which is subsequently solved using a Chapman–Enskog expansion, which examines at a small perturbation around the equilibrium spin polarization density $\overrightarrow{S}$. This gives an expression for the spin current [2, 3], which in conjunction with the equation for precessing spin $\frac{\partial \overrightarrow{S}}{\partial t} + \nabla \cdot \overrightarrow{J} = \gamma \overrightarrow{S} \times \overrightarrow{H}$ leads to the ISR equation for the transverse spin (polarization) density $S_+ = S_x + \mathrm{i}S_y$:

$$\frac{\partial S_+}{\partial t} + \mathrm{i}\gamma H_z S_+ = D_0 \frac{1 - \mathrm{i}\mu\epsilon S_z}{1 + \mu^2 S^2} \nabla^2 S_+,$$

where

D_0 = spin diffusion coefficient
n = gas number density
$\varepsilon = \pm 1$ for bosons/fermions
μ = spin-wave quality factor
S = magnitude of the longitudinal (z) spin polarization
S_+ = transverse spin polarization
H_z = component of $\overrightarrow{H}$ parallel to S
γ = gyromagnetic ratio of the electron or the nucleus.

For a highly polarized gas $S \approx S_z$, and the equation simplifies slightly to

$$\frac{\partial S_+}{\partial t} + \mathrm{i}\gamma H_z S_+ = D_0 \frac{1}{1 + \mathrm{i}\epsilon\mu S} \nabla^2 S_+. \tag{1}$$

This is the ISR equation based on the form given by Lhuillier and Laloë (LL) [2], and is valid for spin- systems with negligible couplings to other degrees of freedom, such as nuclear spins of atoms with 'frozen' electron spins (i.e. the electron spins are fully polarized and the electrons are bound to their respective atoms during collisions).

LL used spin polarization density in their derivation instead of magnetization; further, they chose their axes so that the $S_z(\approx S)$ is always parallel to the positive z-axis. Specifically this means that $0 \leqslant S_z \leqslant 1$. A less obvious consequence is that the sign of γ plays no role in the equation. In particular for electrons $\gamma < 0$, however the spins are aligned against the field. As S_z by definition always points in the positive z-direction, in order for them to be aligned against the magnetic field, one must flip the direction of H_z; this exactly cancels the sign of γ (see also appendix A). Lastly, if one were to flip the polarization/magnetization of the gas, the correct way to account for it in the ISRE equation would be to flip the magnetic field.

Bouchaud and Lhuillier [3] considered atomic hydrogen taking into account both nuclei and electrons (in fact some of their results are general to atoms with one valence electron [22]) and allow electrons to jump from one nucleus to the other during the collision. Specifically they consider the cases of the 0–0 ($F = 0, m_F = 0 - F = 1, m_F = 0$)—coherence in weak magnetic field and the b–c ($S = -1/2$, $I = -1/2$—$S = 1/2$, $I = -1/2$) coherence in strong magnetic field. For both cases they arrive at essentially the same ISR equation but in the former case with a drastically modified quality factor Q, which turns out to significantly limit the observability of 0–0 spin waves:

$$Q = \frac{\mu S_z}{1 + \frac{1 + \mu^2 S_z^2}{D_z k^2} T_2^{-1}}. \tag{2}$$

For the b–c coherence they obtain

$$\frac{\partial z}{\partial t} = \frac{D_z^*(I)}{1 + \mathrm{i}(\mu_1^* M + \mu_2^* S)}\nabla^2 z, \tag{3}$$

where M, S, and I are various quantities characterizing polarization (see section 3.1). This equation has no epsilons (ε) because they are already included in the calculation of the μ and the relationship is not as simple as it is for LL.

Earle [19] considered the spin-1 case of deuterium nuclei and following LL derived the ISR equations for various spin waves, but with μS replaced by $2\mu A_{\pm 2}$ for $\gamma \leftrightarrow \alpha$ transition and $\epsilon\mu(S_0 - \sqrt{6}A_0)$ for $\gamma \leftrightarrow \beta$ spin waves (A_is are the components of the nuclear quadrupolar alignment tensor).

Generally the ISR equation has the form

$$\frac{\partial S_+}{\partial t} = \frac{D_0}{1 + \mathrm{i}\mu_{\mathrm{eff}} S}\nabla^2 S_+ - \mathrm{i}\gamma H_z S_+ \tag{4}$$

with various expressions substituting for μ_{eff} and depending on approach, S may be positive (LL) or assume even negative value (Bouchaud and Lhuillier).

2.1. Trapping magnons

The ISR equation is mathematically similar to Schrödinger equation with magnetic field in the role of potential. While physically the ISR equation is not in any obvious way connected to the energy of spin waves, nonetheless one may use the intuition from the Schrödinger equation to say something about the spin waves. Just as one can speak of trapping quantum systems in a potential, one may also speak of spin waves being trapped by the potential (that is, the magnetic field). Whether the spin waves are attracted to potential minima or maxima depends essentially only on the sign of μ. For example, consider $|\mu| \gg 1$: one may then write the ISR equation as

$$-\mathrm{i}\frac{\mathrm{d}S_+}{\mathrm{d}t} = -\underbrace{\frac{D_0}{\mu}}_{\frac{\hbar^2}{2m}}\nabla^2 S_+ \underbrace{-|\gamma H_z|}_{V(r)} S_+. \tag{5}$$

(Here the modulus of γH_z is used to emphasize the fact that the sign of γ is not relevant.) This differs from a Schrödinger equation only by the sign of $\frac{\mathrm{d}S_+}{\mathrm{d}t}$; taking the complex conjugate would recover a Schrödinger equation for the conjugate S_+^*, a particle with mass $m = \frac{\hbar^2\mu}{2D_0}$. What matters is that the sign of the 'kinetic' term is the same as in Schrödinger equation. Now for $\mu > 0$, a strong magnetic field corresponds to a potential minimum, so the resulting spin waves should concentrate in regions of strong magnetic field. Spin waves in stronger magnetic field would also have higher precession frequency: as the mode number increases, the frequency should decrease as the modes move out of the potential to regions of weaker magnetic field. An increasing frequency spectrum would be observed for $\mu < 0$ or flipped magnetization ($-|\gamma H_z| \to |\gamma H_z|$), but not for a change in the sign of γ as previously explained.

3. The asymptotic expressions

The ISRE parameter μ characterizes the ratio of transverse rotation of ISRE to the normal spin diffusion which tends to homogenize the gas. It depends on three different cross sections (momentum $k = \|\vec{k}\|$): the usual scattering cross section $\sigma_k(\theta)$ of scattered atoms, an interference term $\tau_{\mathrm{fwd}}^{\mathrm{ex}}(k)$ for transmitted atoms, and an interference term for scattered particles $\tau_k^{\mathrm{ex}}(\theta)$ [1]. From these one may obtain the angle-integrated cross sections

$$Q_{[\sigma]}^t(k) = 2\pi\int_0^\pi \sin\theta(1 - \cos^t\theta)\sigma(\theta)\mathrm{d}\theta.$$

The phase shift expansion of the T-matrix gives the expressions of [20]:

$$Q_{[\sigma_k]}^1 = \frac{4\pi}{k^2}\sum_{l=0}^{\infty}(l+1)(\sin(\delta_l - \delta_{l+1}))^2$$

$$Q_{[\tau^{\mathrm{ex}}]}^1 = \frac{8\pi}{k^2}\sum_{l=0}^{\infty}(-1)^l(l+1)\sin(\delta_l - \delta_{l+1})\sin(\delta_l)\sin(\delta_{l+1})$$

$$\tau_{\mathrm{fwd}}^{\mathrm{ex}} = \frac{2\pi}{k^2}\sum_{l=0}^{\infty}(-1)^l(2l+1)\sin(2\delta_l).$$

Here δ_l is the l-wave phase shift. From these, using the collision integrals

$$\Omega_{[\alpha]}^{(t,s)} = \frac{1}{\sqrt{\pi m\beta}}\int_0^\infty \mathrm{e}^{-\gamma^2}\gamma^{2s+3}Q_{[\alpha]}^t\left(k = \sqrt{\frac{m}{\beta}}\frac{\gamma}{\hbar}\right)\mathrm{d}\gamma, \tag{6}$$

$$\Xi_{[\tau_{\mathrm{fwd}}^{\mathrm{ex}}]}^{(s)} = \frac{1}{\sqrt{\pi m\beta}}\int_0^\infty \mathrm{e}^{-\gamma^2}\gamma^{2s+3}\tau_{\mathrm{fwd}}^{\mathrm{ex}}\left(k = \sqrt{\frac{m}{\beta}}\frac{\gamma}{\hbar}\right)\mathrm{d}\gamma, \tag{7}$$

one arrives at the definition of μ:

$$\mu = \frac{\Omega_{[\tau^{\mathrm{ex}}]}^{(1,1)} + \Xi_{[\tau_{\mathrm{fwd}}^{\mathrm{ex}}]}^{(1)}}{\Omega_{[\sigma_k]}^{(1,1)}}.$$

Assuming that for low momenta the phase shift behaves asymptotically as $\delta_l = -(ka_l)^{2l+1} + n\pi$ justifies the definition of the l-wave scattering length:

$$a_l = -\left(\lim_{k\to 0}\frac{\tan(\delta_l(k))}{k^{2l+1}}\right)^{\frac{1}{2l+1}}.$$

For $l = 0$, 1 this usually works, but for higher partial waves the scattering length defined thus may not be finite. However, the phase shift may behave as $\sim(ka_l)^q$ for some q, in which case higher scattering lengths may be defined by suitably adjusting the definition of the phase shift.

Expanding the angle-averaged quantities to second order in k gives

$$Q_{[\sigma_k]}^1 = 4\pi a_0^2 - 4\pi a_0 k^2\left(\frac{a_0^3}{3} + 2a_1^3\right) + \mathcal{O}(k^4), \tag{8}$$

$$Q_{[\tau^{\mathrm{ex}}]}^1 = \mathcal{O}(k^3)$$

$$\tau_{\mathrm{fwd}}^{\mathrm{ex}} = -\frac{4\pi a_0}{k} + 4\pi k\left(\frac{2}{3}a_0^3 + 3a_1^3\right) + \mathcal{O}(k^3). \tag{9}$$

One could also take terms up to first-order in k, but most likely owing to the rational form of μ these seem to be less accurate. Higher-order terms may depend on a_2 which, as mentioned before, generally is not finite, and one may have to

consider the sign of $Q^1_{[\tau^{\rm ex}_{\rm fwd}]}$ due to $n\pi$ term of δ_l, which turns out not to be an issue for $Q^1_{[\sigma_k]}$ (square of sine) and $\tau^{\rm ex}_{\rm fwd}$ (always a multiple of 2π).

In the next step the above expressions are integrated with a Gaussian over all k. The validity of this approximation is discussed in appendix B. The results are

$$\Omega^{(1,1)}_{[\sigma_k]} = 4\pi a_0^2 - \frac{4\pi a_0^4 m}{\beta\hbar^2} - \frac{24\pi a_0 m}{\beta\hbar^2} a_1^3$$
$$\Xi^{(1)}_{[\tau^{\rm ex}_{\rm fwd}]} = -\frac{3\pi^{\frac{3}{2}} a_0 \hbar}{2\sqrt{m}}\sqrt{\beta} + \frac{5\pi^{\frac{3}{2}} a_0^3\sqrt{m}}{2\sqrt{\beta}\hbar} + \frac{45\pi^{\frac{3}{2}} a_1^3\sqrt{m}}{4\sqrt{\beta}\hbar}.$$

Taking the first term of both expressions (with $\Lambda = \sqrt{\frac{h^2\beta}{2\pi m}}$), the asymptotic behavior is

$$\mu = -\frac{3\sqrt{2}}{16}\left(\frac{\Lambda}{a_0}\right). \tag{10}$$

The same result was obtained earlier in [18]. As can be seen, the sign of μ at low temperatures is determined by the s-wave scattering length.

Using all the terms of the collision integrals above, one arrives at the first-order μ:

$$\mu = -\frac{-3\sqrt{2}\Lambda^3}{16\Lambda^2 a_0 - 32\pi a_0^3 - 192\pi a_1^3} + \frac{5\sqrt{2}\pi\Lambda a_0^2}{8\Lambda^2 a_0 - 16\pi a_0^3 - 96\pi a_1^3} + \frac{45\sqrt{2}\pi\Lambda a_1^3}{16 a_0(\Lambda^2 a_0 - 2\pi a_0^3 - 12\pi a_1^3)}. \tag{11}$$

3.1. Asymptotic behavior of μ in Bouchaud and Lhuillier's treatment of b–c coherence in atomic hydrogen

Bouchaud and Lhuillier's treatment of the ISRE problem is far more detailed as compared to LLs, and as a result the calculations are even more cumbersome. The expressions for the μ^* factors in (3) are given by the following formulae:

$$\begin{aligned} D_0 = {} & \left[\frac{8nm}{3kT}\right]\Bigg[\Omega^{(1,1)}_{[\sigma_d]} - \left(\frac{1+I}{2}\right)\Omega^{(1,1)}_{[\sigma_{dt}]} \\ & + (1-I)\Omega^{(1,1)}_{[\sigma^{\rm ex}_{dt}]} - \tilde{\Omega}^{(1,0)}_{[\sigma^{\rm ex}_{dt}]} + \frac{1}{2}\tilde{\Omega}^{(0,0)}_{[\sigma_t]} \\ & + (1-I)\tilde{\Omega}^{(1,0)}_{[\sigma^{\rm ex}_t]} + \frac{3I}{2}\Omega^{(1,0)}_{[\sigma^{\rm ex}_t]} + \left[\frac{1-I}{2}\right]\Omega^{(1,1)}_{[\sigma^{\rm ex}_d]}\Bigg] \\ \frac{\mu_1^*}{D_0} = {} & \left[\frac{8nm}{6kT}\right][\Xi^1_{\tau^{\rm bwd}_d} - \tilde{\Omega}^{(1,1)}_{[\tau^{\rm ex}_d]} - \tilde{\Omega}^{(1,1)}_{[\tau^{\rm ex}_t]} \\ & + 3\Xi^0_{\tau^{\rm fwd}_t} - \Xi^1_{\tau^{\rm fwd}_t} + 6\tilde{\Omega}^{(0,0)}_{[\tau_{dt}]} - 2\tilde{\Omega}^{(1,1)}_{[\tau_{dt}]}] \\ \frac{\mu_2^*}{D_0} = {} & -\left[\frac{8nm}{6kT}\right][\Xi^1_{\tau^{\rm bwd}_t} + 3\Xi^0_{\tau^{\rm fwd}_t} \\ & + 2\tilde{\Omega}^{(1,1)}_{[\tau_{dt}]} + 6\tilde{\Omega}^{(0,0)}_{[\tau_{dt}]}]. \end{aligned} \tag{12}$$

The quantities in the formulae are similar to those used in the previous section. A more comprehensive summary is given in appendix C and supplementary material[4].

[4] See supplemental material at stacks.iop.org/PS/93/094002/mmedia for details of the derivations.

Using the SymPy Python package [23] to perform the expansions to first-order, the expressions for the μs one obtains are

$$\mu_1^* = -\frac{3\sqrt{2}\Lambda a_g}{4Ia_g^2 - 16Ia_g a_u - 4Ia_u^2 + 10a_g^2 + 4a_g a_u + 34a_u^2}, \tag{13}$$

$$\mu_2^* = \frac{9\sqrt{2}\Lambda(a_g - a_u)}{8Ia_g^2 - 32Ia_g a_u - 8Ia_u^2 + 20a_g^2 + 8a_g a_u + 68a_u^2}, \tag{14}$$

$$\mu = M\mu_1^* + S\mu_2^* \tag{15}$$

with

$$I = \frac{n_a + n_d - n_b - n_c}{n} \quad \text{(nuclear polarization)}$$
$$S = \frac{n_d + n_c - n_a - n_b}{n} \quad \text{(electron polarization)}$$
$$M = \frac{n_c - n_b}{n}.$$

a_g and a_u correspond to singlet and triplet potential scattering lengths, and the n_i ($i = a, b, c, d$) being the number density of each spin state of atomic hydrogen in strong fields. For a gas consisting of pure b-state, $I = S = M = -1$ and one obtains

$$\mu = -\mu_1^* - \mu_2^* = -\left(-\frac{3\sqrt{2}\Lambda a_{g,0}}{6a_{g,0}^2 + 20a_{g,0}a_{u,0} + 38a_{u,0}^2} + \frac{9\sqrt{2}\Lambda(a_{g,0} - a_{u,0})}{12a_{g,0}^2 + 40a_{g,0}a_{u,0} + 76a_{u,0}^2}\right).$$

To compare with LL we artificially set $a_{g,0} = 0$: one is left with $-\left(-\frac{9\sqrt{2}\Lambda}{76a_{u,0}}\right) \approx 0.12\frac{\sqrt{2}\Lambda}{a_{u,0}}$, to be compared with LL's $\varepsilon\mu S \approx -0.19\frac{\sqrt{2}\Lambda}{a_0}$.

4. Comparison of exact and asymptotic curves for μ

Figures 1 and 2 show μ calculated for hydrogen's triplet potential ($b^3\sigma_u^+$) and ^{3}He. The figures also show a comparison between the asymptotic formulae and more comprehensive calculations in the fashion of [20] ('exact'). A trend that seems to emerge from these examples is that the first-order expression differs more from the exact result than the zeroth-order asymptotic formula. Given the poorness of the results especially for ^{3}He, it seems likely that the first-order formula is a poor approximation of μ, though it remains possible it is the 'exact' μ which is inaccurate.

For hydrogen, a refined Kolos–Wolniewicz potential [24] was used to calculate $a_0^u = 0.71$ Å and $a_1^u = -2.70$ Å with the variable phase method [25]; the results are in good agreement with other calculations [26]. For the singlet scattering length in the Bouchaud and Lhuillier approximation, $a_0^g = 0.16$Å was used [27]. The required phase shift curves for the 'exact' μ were calculated using a combination of the variable phase method and a version of the usual

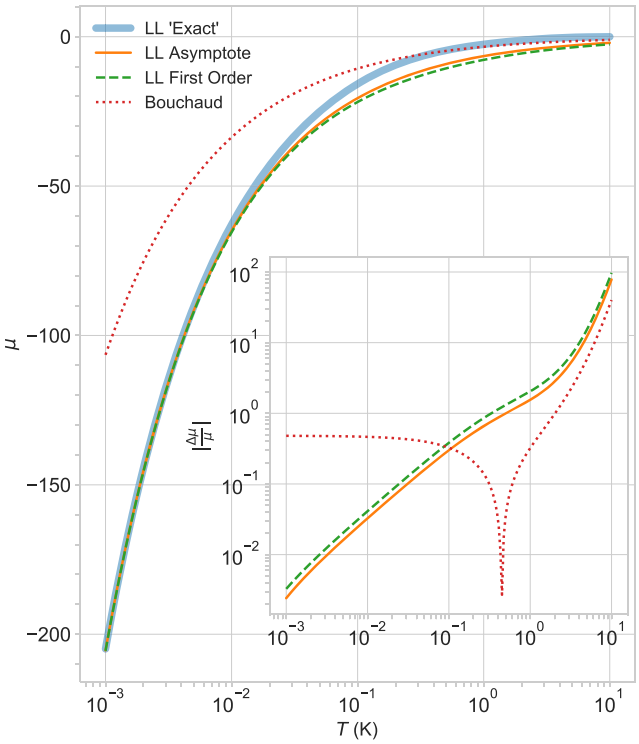

Figure 1. Accuracy of the asymptotic approximations for hydrogen. The figure shows the 'exact' calculation, the asymptotic formula equation (10), the first-order formula equation (11), and the asymptotic Bouchaud formula equation (15) for μ in hydrogen. The inset shows the relative error from the 'exact' value. The discrepancy is around 30% for $T \sim 0.1$ K for the LL formulae. The Bouchaud and Lhuillier formula ($\mu = \mu_1^* + \mu_2^*$) differs more at low temperatures.

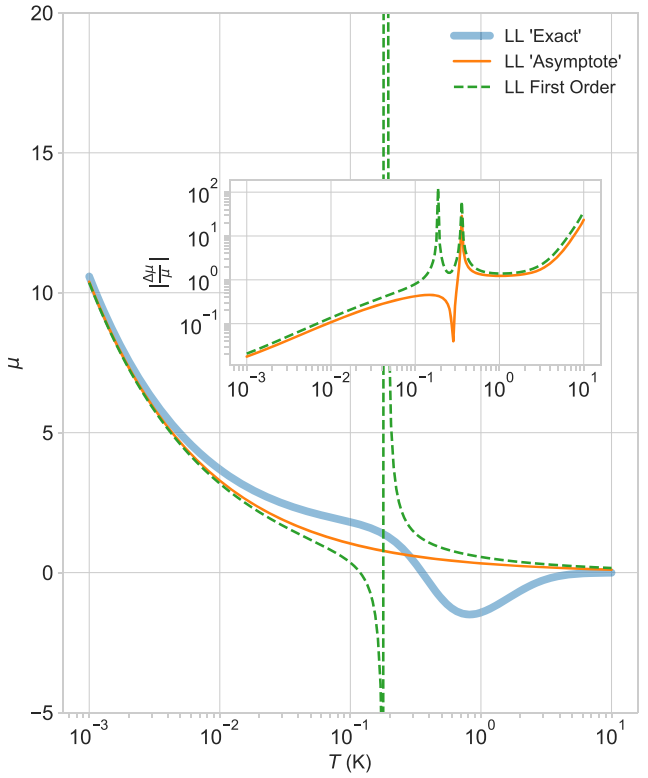

Figure 2. Accuracy of the asymptotic approximations for ^{3}He. The figure shows the 'exact' calculation, the asymptotic formula equation (10), and the first-order formula equation (11) μ in ^{3}He. The inset shows the relative error from the 'exact' value. The discrepancy is around 10% for $T \sim 0.01$ K. μ changes sign which leads to the divergence of the first-order result.

solution-matching method [28]. The resulting asymptotic and first-order curves are seen to follow the 'exact' curve, although the relative discrepancy even at 0.1 K is around 30% for both. Further, the first-order expression is clearly less accurate. The Bouchaud and Lhuillier formula $\mu = \mu_1^* + \mu_2^*$ fares better at higher temperatures (above 0.1 K) compared to either LL results. However the situation changes at about 0.1 K where the asymptotic Bouchaud and Lhuiller curve departs from the other curves. On one hand this speaks of the applicability of the LL treatment in many contexts, on the other hand it shows that Bouchaud's more detailed approach differs from the more general treatment of LL to a degree which cannot be explained by the LL theory. In particular it would seem to suggest differences between electron spin waves (b–c-coherence) and nuclear spin waves (a–d-coherence) in hydrogen. With Bouchaud and Lhuillier's definition of $M < 0$ for hydrogen gas in pure b-state and LL's definition $M > 0$ always, the $\mu_{\text{eff}}\, M$ should have different sign for these two approaches.

For ^{3}He, $a_0 = -8.0592$ Å and $a_1 = -3.024$ Å, calculated from a Lennard-Jones potential [20]. Once again both curves approximate the 'exact' result equally well until the discontinuity; there the asymptotic formula fares better though neither correctly approximates the behavior. A summary of scattering length used in this work is presented in Table 1 of Appendix B.

5. Conclusions

We derived asymptotic expressions for the quality factor of the ISRE nuclear spin waves in quantum gases of atomic hydrogen and ^{3}He using the theory of LL based on scattering of identical particles with spin-$\frac{1}{2}$. For electron spin waves in atomic hydrogen we used the more accurate treatment of Bouchaud and Lhuillier where the true four-particle nature of the scattering (two electrons, two nuclei) is considered. The quality factor parameter μ was calculated with first and second order approximations. Comparing the asymptotic values of μ with results of exact numerical calculations we found that they agree well with each other within the experimentally accessible range of temperatures 0.1–1 K, and diverge at low temperatures as Λ/a_0.

Reminiscences from Kalle-Antti Suominen: I first met Wolfgang in 1988 at a small meeting in Finland, organized by Stig Stenholm, and later we met several times at different occasions. Among the most memorable ones was the PhD thesis defense of Dr Asta Paloviita in Helsinki, when my task was to get Wolfgang into the official academic attire, namely a tailcoat or 'frack'. He made quite an impressive and handsome sight. I also had the pleasure to visit him and Cathy at Ulm, where they took me to see the famous Neuschwanstein castle in Bavaria. Wolfgang was also one of the key

speakers at the CEWQO2009 conference in Turku, where we both honored the 70th birthday of our friend and colleague Stig Stenholm, to whom we both have many reasons to be thankful (sadly, Stig passed away in 2017). Wolfgangs scientific interests have been both broad and deep, and his writings have had an essential impact on my research as well as on my lectures on quantum optics. Together with my colleagues in Turku, I congratulate Wolfgang on his 60th birthday.

Acknowledgments

LL is supported by the Vilho, Yrjö and Kalle Väisälä Foundation of the Finnish Academy of Science and Letters. This work was also supported by the Academy of Finland (grants nos. 122595 and 133682), the Wihuri Foundation and by NSF Grant No. DMR 1707565.

Appendix A. The effect of the sign of γ

Assuming the time dependence of ISRE spin waves to be given by $e^{i\Omega t}$ (with Ω generally being a complex number), equation (4) becomes

$$i\Omega S_+ = \frac{D_0}{1 \pm i\mu_{\rm eff}}\nabla^2 S_+ - i\gamma H_z S_+. \tag{A1}$$

To make explicit the dependence of S on γ we substitute $S = \frac{2}{\gamma\hbar}M$; the substitution cancels out everywhere but the denominator on the right

$$i\Omega M_+ = \frac{D_0\gamma\hbar}{\hbar\gamma \pm 2i\mu_{\rm eff}M}\nabla^2 M_+ - i\gamma H_z M_+. \tag{A2}$$

Substituting $\gamma \to -\gamma$ leads to

$$i\Omega M_+ = \frac{-D_0\gamma\hbar}{-\hbar\gamma \pm 2i\mu_{\rm eff}M}\nabla^2 M_+ + i\gamma H_z M_+ \tag{A3}$$

$$= \frac{D_0\gamma\hbar}{\hbar\gamma \mp 2i\mu_{\rm eff}M}\nabla^2 M_+ + i\gamma H_z M_+. \tag{A4}$$

Then we take the complex conjugate:

$$\overbrace{i(-\Omega^*)}^{\widetilde{\Omega}} M_+^* = \frac{D_0\gamma\hbar}{\hbar\gamma \pm 2i\mu_{\rm eff}M}\nabla^2 M_+^* - i\gamma H_z M_+^*. \tag{A5}$$

The equation we have arrived at is exactly equation (A1) for $\widetilde{\Omega}$, so the solutions must be the same, with $\widetilde{\Omega} = \omega + \frac{i}{\tau}$ for $\omega, \tau \geqslant 0$, and time dependence $e^{-\frac{t}{\tau}+i\omega t}$. The solutions of the original equation must then have $\Omega = -\widetilde{\Omega}^* = -\omega + \frac{i}{\tau}$ and time dependence $e^{-\frac{t}{\tau}-i\omega t}$; this is merely a reversal of the precession direction.

Appendix B. Validity of the asymptotic expression

Various approximations were made in the course of the deriving the asymptotic expressions and first-order expressions. The finiteness and the asymptotic form the of the scattering phase shift has already been alluded to. Immediately following is the approximation of the sine by its Taylor expansion. Note that the argument being approximated is not only the phase shift, but it can also be a difference of phase shifts. This does not essentially change the situation: the factors of π cancel out within the sine, and the remaining quantities are small for small k.

The region of validity for these approximations is shown in figure B1 for hydrogen. The figure compares equations (8) and (9) with the numerically evaluated expressions for $Q^1_{[\sigma_k]}$ and $\tau^{\rm ex}_{\rm fwd}$; $Q^1_{[\tau^{\rm ex}]}$ is also shown for completeness. The approximations are clearly robust for $k < 1 \times 10^{-2}\,\text{Å}^{-1}$, beyond which they begin to deteriorate. In the good regime, then, the following conditions should hold

$$4\pi k^2 \left| a_0\left(\frac{a_0^3}{3} + 2a_1^3\right)\right| \ll 4\pi a_0^2 \Leftrightarrow k^2 \ll \frac{3|a_0|}{|a_0^3 + 6a_1^3|}, \tag{B1}$$

$$4\pi k \left|\frac{2}{3}a_0^3 + 3a_1^3\right| \ll \left|\frac{4\pi a_0}{k}\right| \Leftrightarrow k^2 \ll \frac{3|a_0|}{|2a_0^3 + 9a_1^3|}. \tag{B2}$$

For $\tau^{\rm ex}_{\rm fwd}$, $-\frac{4\pi a_0}{k}$ seems to remain a good approximation even beyond the point where the k term begin to depart from the approximation (at the turn of the asymptotic formula). Combined with the overwhelming magnitude of $\tau^{\rm ex}_{\rm fwd}$ this may explain why the asymptotic formula remains robust for hydrogen even beyond the region where these approximations break down.

In the next step an integration over all momenta is carried out. Obviously this is in contradiction with the small k approximation needed for the preceding approximations. However, the functions being integrated have a Gaussian form, so for suitable parameter regimes the contributions from higher momenta are negligible. In general the integrals in equations (6) and (7) depend on the scaled momentum γ as $e^{-\gamma^2}\gamma^q$; they are shown for a few temperatures in figure B1 ($q = 5$). For 1 K the approximations are already not that good, but in fact for hydrogen the approximations seem to be valid below 0.01 K.

Clearly what is needed is for the Gaussian to be centered at a region where the approximations hold. $e^{-\gamma^2}\gamma^q$ is centered at $\gamma^* = \sqrt{\frac{q}{2}} = \sqrt{\frac{5}{2}}$, giving $(k^*)^2 = \frac{5m}{2\beta\hbar^2}$, which should be smaller than the momentum where the approximations break down. Combining this with equations (B1) and (B2) results in two conditions for temperature:

$$T \ll \frac{6\hbar^2|a_0|}{5mk_B|a_0^3 + 6a_1^3|} = T_Q, \tag{B3}$$

$$T \ll \frac{6\hbar^2|a_0|}{5mk_B|2a_0^3 + 9a_1^3|} = T_\tau. \tag{B4}$$

T_τ is almost always the smaller of the two, except in the narrow region where $-5^{\frac{1}{3}} < \frac{a_0}{a_1} < -3^{\frac{1}{3}}$. Numerical evaluations of the upper bounds T_Q and T_τ for hydrogen and ^{3}He are presented in Table 1.

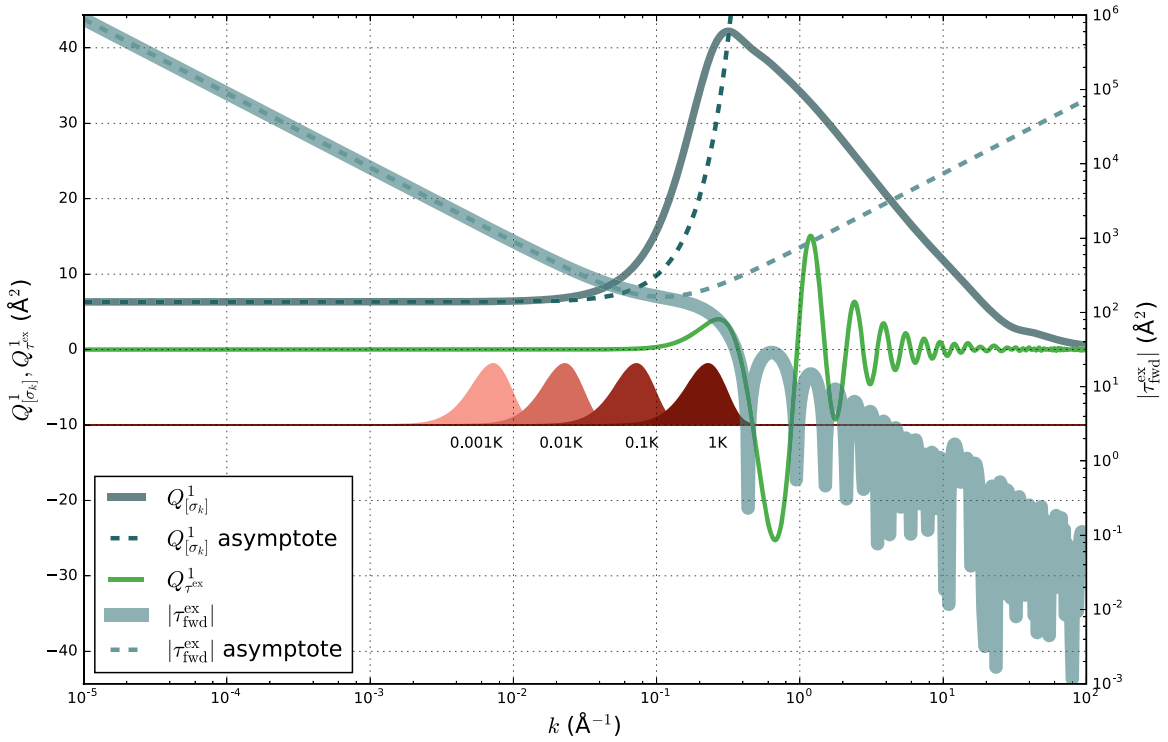

Figure B1. Accuracy of approximations at different momenta/temperatures. The figure shows $Q^1_{[\sigma_k]}$, τ^{ex}_{fwd} for atomic hydrogen with their series expansions equations (8) and (9), as well as $Q^1_{[\tau^{ex}]}$. These quantities are multiplied with a Gaussian and integrated over all momenta; a few Gaussians for a few different temperatures are shown. For high enough momenta the series expansions naturally break down, so in order for the asymptotic formula to give a good approximation to μ the Gaussian should be concentrated in the area where the series expansions approximate the quantities well. This gives upper bounds T_Q and T_τ on temperature where the asymptotic formula can be expected to work.

Table 1. Small k regimes s-wave and p-wave scattering lengths and the temperature upper bounds T_Q and T_τ (equations (B3) and (B4)) for validity of asymptotic formula for a few atomic species under the triplet potential interaction. T_Λ is derived from the quantum gas criterion $\frac{\Lambda_{th}}{|a_s|} > 1$ and is shown for comparison.

Species	a_0	a_1	T_Q	T_τ	T_Λ
H	0.71 Å	−2.70 Å	0.34 K	0.23 K	600 K
^{3}He	−8.1 Å	−3.024 Å	0.22 K	0.11 K	1.54 K

Appendix C. A dictionary of cross sections

This section largely reproduces definitions and results from [3]. However as [3] does not give all the required quantities, some of them are derived in the supplementary material (see footnote 4).

Equations (6) and (7) define Ω and Ξ. In addition another angular average needs to be defined:

$$\tilde{Q}^t_{[\sigma]} = 2\pi \int_0^\pi \sin\theta \sigma(\theta) \mathrm{d}\theta. \tag{C1}$$

$\tilde{\Omega}$ uses this quantity instead of Q; further

$$Q^t_{[\sigma]} = \widetilde{Q}^0_{[\sigma]} - \widetilde{Q}^t_{[\sigma]}. \tag{C2}$$

What remains is to list the relevant cross sections and angular averages Q in equation (12). Some of these are given in [3]; in addition changes between quantities $\sigma \leftrightarrow \sigma^{ex}$ can be easily done with the substitution $(2L+1) \leftrightarrow (-1)^L(2L+1)$. The rest of the derivations are presented in the see supplementary material (see footnote 4). The u and g indices in these expressions stand for phase shifts calculated from the triplet and single potentials of hydrogen, respectively.

$$\tilde{Q}^0_{[\sigma_t]} = \frac{\pi}{k^2}\sum_L (2L+1)\sin^2(\delta^g_L - \delta^u_L)$$

$$\tilde{Q}^0_{[\sigma^{ex}_t]} = \frac{4\pi}{k^2}\sum_L (-1)^L(2L+1)\sin^2(\delta^g_L - \delta^u_L)$$

$$\tilde{Q}^0_{[\sigma_d]} = \frac{\pi}{k^2}\sum_L (2L+1) \times [\sin^2\delta^g_L + \sin^2\delta^u_L + 2\cos(\delta^u_L - \delta^g_L)\sin\delta^u_L \sin\delta^g_L]$$

$$\tilde{Q}^0_{[\sigma^{ex}_d]} = \frac{\pi}{k^2}\sum_L (-1)^L(2L+1) \times [\sin^2\delta^g_L + \sin^2\delta^u_L + 2\cos(\delta^u_L - \delta^g_L)\sin\delta^u_L \sin\delta^g_L]$$

$$\tilde{Q}^0_{[\sigma_{dt}]} = \frac{\pi}{k^2}\sum_L (2L+1)[\sin^2\delta^g_L - \sin^2\delta^u_L]$$

$$\tilde{Q}^0_{[\sigma^{ex}_{dt}]} = \frac{\pi}{k^2}\sum_L (-1)^L(2L+1)[\sin^2\delta^g_L - \sin^2\delta^u_L]$$

$$\tilde{Q}^1_{[\sigma_{dt}]} = \frac{4\pi}{k^2}\sum_L (L+1)[\sin(\delta^u_{L+1})\sin(\delta^g_L)\sin(\delta^g_L - \delta^u_{L+1}) + \sin(\delta^u_L)\sin(\delta^g_{L+1})\sin(\delta^g_{L+1} - \delta^u_L)]$$

$$\tilde{Q}^{1}_{[\sigma^{\rm ex}_{dt}]} = \frac{4\pi}{k^2}\sum_L (-1)^L (L+1)[\sin(\delta^u_{L+1})\sin(\delta^g_L)\sin(\delta^g_L - \delta^u_{L+1}) + \sin(\delta^u_L)\sin(\delta^g_{L+1})\sin(\delta^g_{L+1} - \delta^u_L)]$$

$$Q^{0}_{[\sigma^{\rm ex}_t]} \equiv \tilde{Q}^{0}_{[\sigma^{\rm ex}_t]}$$

$$Q^{1}_{[\sigma_d]} = \tilde{Q}^{0}_{[\sigma_d]} - \tilde{Q}^{1}_{[\sigma_d]} = \tilde{Q}^{0}_{[\sigma_d]} - 0$$

$$Q^{1}_{[\sigma^{\rm ex}_d]} = \tilde{Q}^{0}_{[\sigma^{\rm ex}_d]} - \tilde{Q}^{1}_{[\sigma^{\rm ex}_d]} = \tilde{Q}^{0}_{[\sigma^{\rm ex}_d]} - 0$$

$$Q^{1}_{[\sigma_{dt}]} = \tilde{Q}^{0}_{[\sigma_{dt}]} - \tilde{Q}^{1}_{[\sigma_{dt}]}$$

$$Q^{1}_{[\sigma^{\rm ex}_{dt}]} = \tilde{Q}^{0}_{[\sigma^{\rm ex}_{dt}]} - \tilde{Q}^{1}_{[\sigma^{\rm ex}_{dt}]}$$

$$\tilde{Q}^{0}_{[\tau_{dt}]} = \frac{2\pi}{k^2}\sum_L (2L+1)\sin(\delta^g_L)\sin(\delta^u_L)\sin(\delta^g_L - \delta^u_L)$$

$$\tilde{Q}^{1}_{[\tau_{dt}]} = \frac{2\pi}{k^2}\sum_L (L+1)[\sin(\delta^g_L)\sin(\delta^g_{L+1})\sin(\delta^g_{L+1} - \delta^g_L) - \sin(\delta^u_L)\sin(\delta^u_{L+1})\sin(\delta^u_{L+1} - \delta^u_L)]$$

$$\tilde{Q}^{1}_{[\tau^{\rm ex}_t]} = \frac{2\pi}{k^2}\sum_L (-1)^L (L+1)[\sin(\delta^u_L)\sin(\delta^u_{L+1})\sin(\delta^u_{L+1} - \delta^u_L) + \sin(\delta^g_L)\sin(\delta^g_{L+1})\sin(\delta^g_{L+1} - \delta^g_L) - \sin(\delta^g_L)\sin(\delta^u_{L+1}) \times \sin(\delta^u_{L+1} - \delta^g_L) - \sin(\delta^u_L)\sin(\delta^g_{L+1})\sin(\delta^g_{L+1} - \delta^u_L)]$$

$$\tilde{Q}^{1}_{[\tau^{\rm ex}_d]} = \frac{2\pi}{k^2}\sum_L (-1)^L (L+1)[\sin(\delta^u_L)\sin(\delta^u_{L+1})\sin(\delta^u_{L+1} - \delta^u_L) + \sin(\delta^g_L)\sin(\delta^g_{L+1})\sin(\delta^g_{L+1} - \delta^g_L) + \sin(\delta^g_L)\sin(\delta^u_{L+1}) \times \sin(\delta^u_{L+1} - \delta^g_L) + \sin(\delta^u_L)\sin(\delta^g_{L+1})\sin(\delta^g_{L+1} - \delta^u_L)]$$

$$\tau^{\rm fwd}_t = \frac{\pi}{k^2}\sum_L (2L+1)(\sin(2\delta^g_L) - \sin(2\delta^u_L))$$

$$\tau^{\rm bwd}_d = \frac{\pi}{k^2}\sum_L (-1)^L (2L+1)(\sin(2\delta^g_L) + \sin(2\delta^u_L))$$

$$\tau^{\rm bwd}_t = \frac{\pi}{k^2}\sum_L (-1)^L (2L+1)(\sin(2\delta^g_L) - \sin(2\delta^u_L)).$$

ORCID iDs

L Lehtonen https://orcid.org/0000-0001-7865-9655

References

[1] Lhuillier C and Laloë F 1982 *J. Phys.* **43** 197–224
[2] Lhuillier C and Laloë F 1982 *J. Phys.* **43** 225–41
[3] Bouchaud J P and Lhuillier C 1985 *J. Phys.* **46** 1781–95
[4] Johnson B R, Denker J S, Bigelow N, Lévy L P, Freed J H and Lee D M 1984 *Phys. Rev. Lett.* **52** 1508–11
[5] Bigelow N P, Freed J H and Lee D M 1989 *Phys. Rev. Lett.* **63** 1609–12
[6] Vainio O, Ahokas J, Novotny S, Sheludyakov S, Zvezdov D, Suominen K A and Vasiliev S 2012 *Phys. Rev. Lett.* **108** 185304
[7] Vainio O *et al* 2015 *Phys. Rev. Lett.* **114** 125304
[8] Corruccini L R, Osheroff D D, Lee D M and Richardson R C 1971 *Phys. Rev. Lett.* **27** 650–3
[9] Nacher P, Tastevin G, Leduc M, Crampton S and Laloë F 1984 *J. Phys. Lett.* **45** 441–8
[10] Tastevin G, Nacher P, Leduc M and Laloë F 1985 *J. Phys. Lett.* **46** 249–54
[11] Gully W J and Mullin W J 1984 *Phys. Rev. Lett.* **52** 1810–3
[12] Fuchs J, Gangardt D and Laloë F 2002 *Phys. Rev. Lett.* **88** 230404
[13] Deutsch C, Ramirez-Martinez F, Lacroûte C, Reinhard F, Schneider T, Fuchs J N, Piéchon F, Laloë F, Reichel J and Rosenbusch P 2010 *Phys. Rev. Lett.* **105** 020401
[14] Maineult W, Deutsch C, Gibble K, Reichel J and Rosenbusch P 2012 *Phys. Rev. Lett.* **109** 020407
[15] Leggett A J and Rice M J 1968 *Phys. Rev. Lett.* **20** 586–9
[16] Leggett A J 1970 *J. Phys. C: Solid State Phys.* **3** 448
[17] Bashkin E P 1981 *JETP Lett.* **33** 8
[18] Miyake K, Mullin W and Stamp P 1985 *J. Phys.* **46** 663–71
[19] Earle K, Freed J and Lee D 1992 *J. Low Temp. Phys.* **89** 911–37
[20] Lhuillier C 1983 *J. Phys.* **44** 1–12
[21] Pinard M and Laloë F 1980 *J. Phys.* **41** 769–97
[22] Bouchaud J P and Lhuillier C 1985 *J. Phys.* **46** 1101–12
[23] Meurer A *et al* 2017 *Peer J. Comput. Sci.* **3** e103
[24] Jamieson M, Dalgarno A and Wolniewicz L 2000 *Phys. Rev.* A **61** 1–6
[25] Calogero F 1967 Variable phase approach to potential scattering *Mathematics in Science and Engineering* ed F Calogero vol 35 (Elsevier) pp 67–84
[26] Joudeh B 2013 *Physica* B **421** 41–5
[27] Jamieson M J, Cheung A S C and Ouerdane H 2010 *Eur. Phys. J.* D **56** 181–8
[28] Wei H and Le Roy R J 2006 *Mol. Phys.* **104** 147–50